Pyridine functionalized N-heterocyclic silane complexes of iridium and rhodium – an unexpected change in coordination

Felix Kaiser,[a,b] Robert M. Reich,[a] Eric Rivard[b] and Fritz. E. Kühn[a]*

a. Catalysis Research Center and Department of Chemistry, Technische Universität München, Molecular Catalysis and Wacker Institute, Lichtenbergstr. 4, 85747 Garching bei München, Germany. E-Mail: fritz.kuehn@ch.tum.de

b. Department of Chemistry, University of Alberta, 11227 Saskatchewan Dr., Edmonton, Alberta Canada, T6G 2G2. E-mail: erivard@ualberta.ca.

- Supporting Information -

Table of Contents
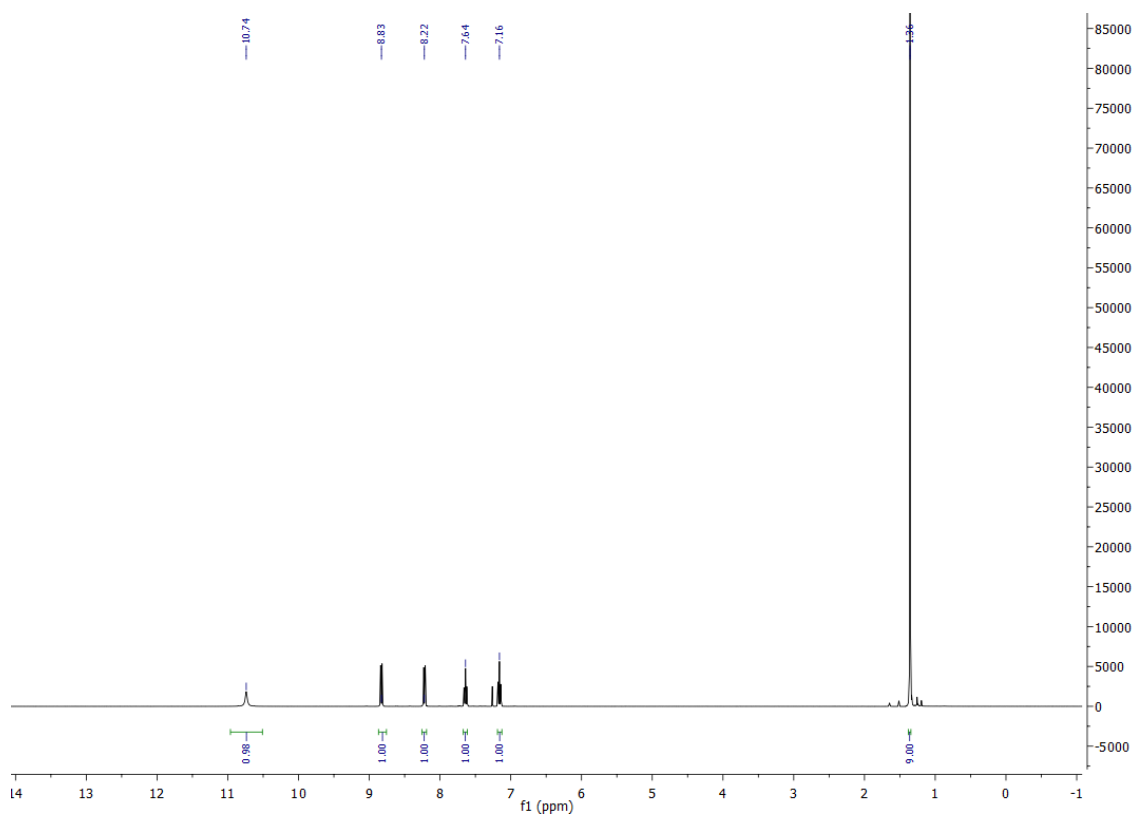
1. NMR spectroscopy

a) ^{1}H NMR

Figure S1: ^{1}H NMR spectrum of N-(2-nitrophenyl) pivalamide (**1**).
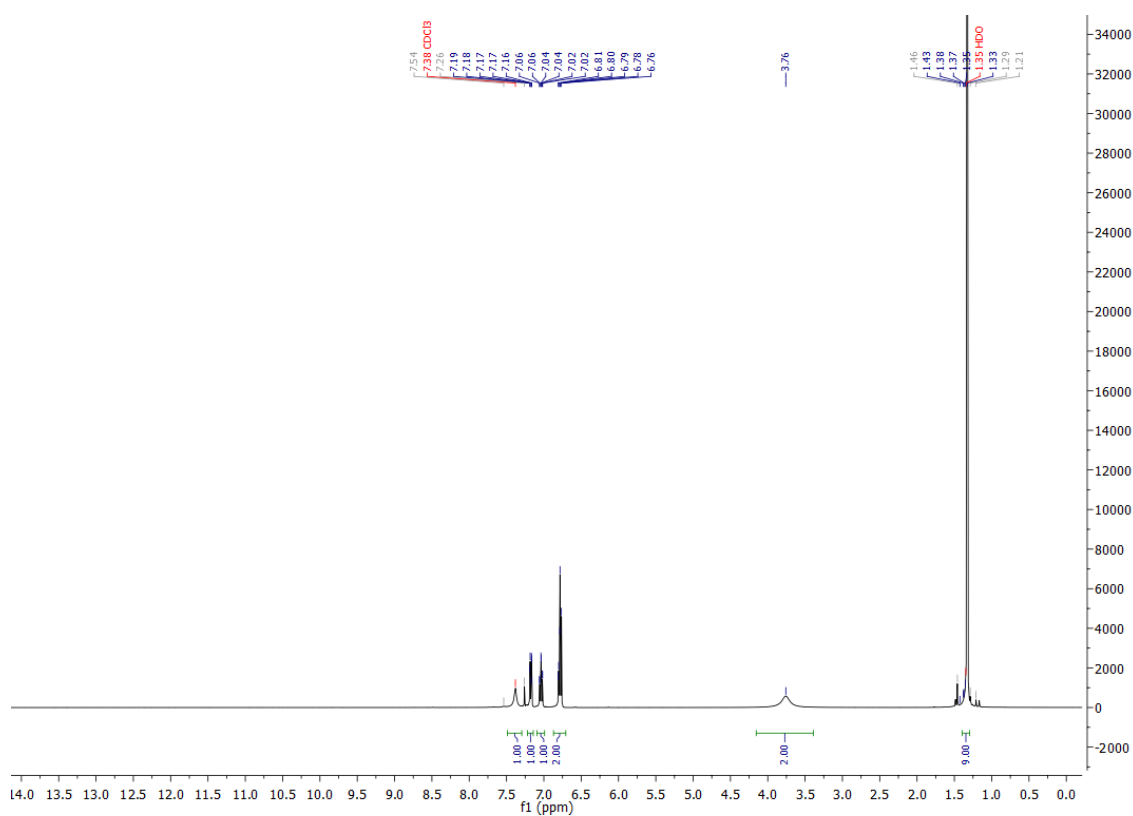
Figure S2: ^{1}H NMR spectrum of *N*-(2-aminophenyl) pivalamid (**2**).

Figure S3: ^{1}H NMR spectrum of N-neopentyl-N'-(pyridin-2-ylmethyl) phenylene diamine (**3**).

Figure S4: ^{1}H NMR spectrum of 1-neopentyl-2,2-hydrochloro-3-((pyridin-2-yl)-methyl)-benzo[1,3,2] diazasilol (**4**).
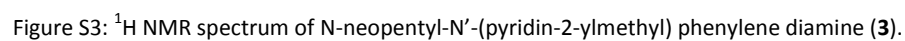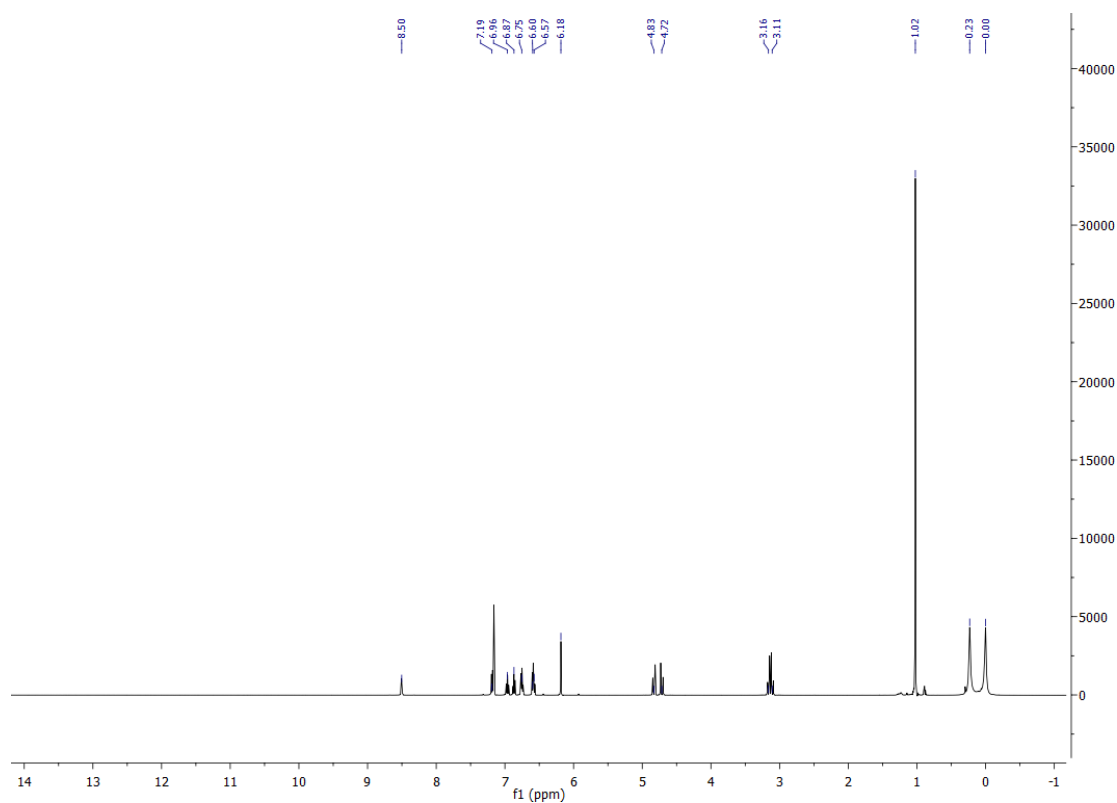
Figure S5: ^{1}H NMR spectrum of 1-neopentyl-2-hydro-2-(bis-trimethylsilylamido)-3-((pyridin-2-yl)-methyl)-benzo[1,3,2] diazasilol (**5**).
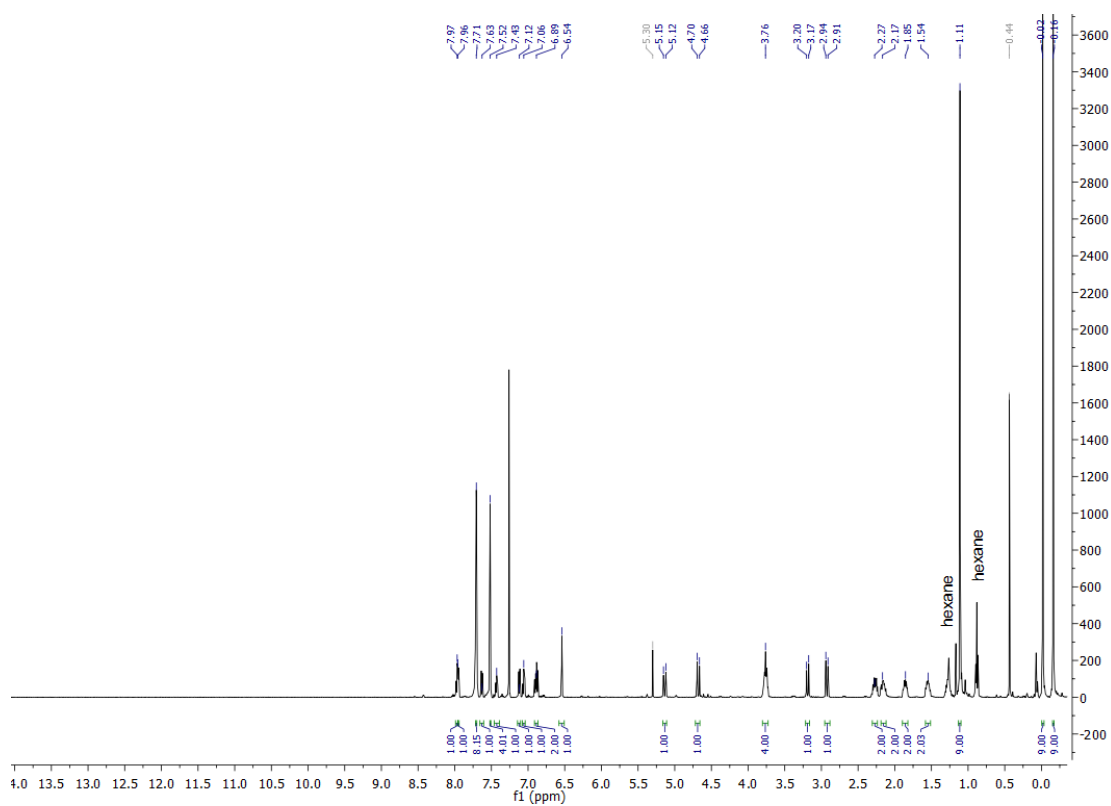

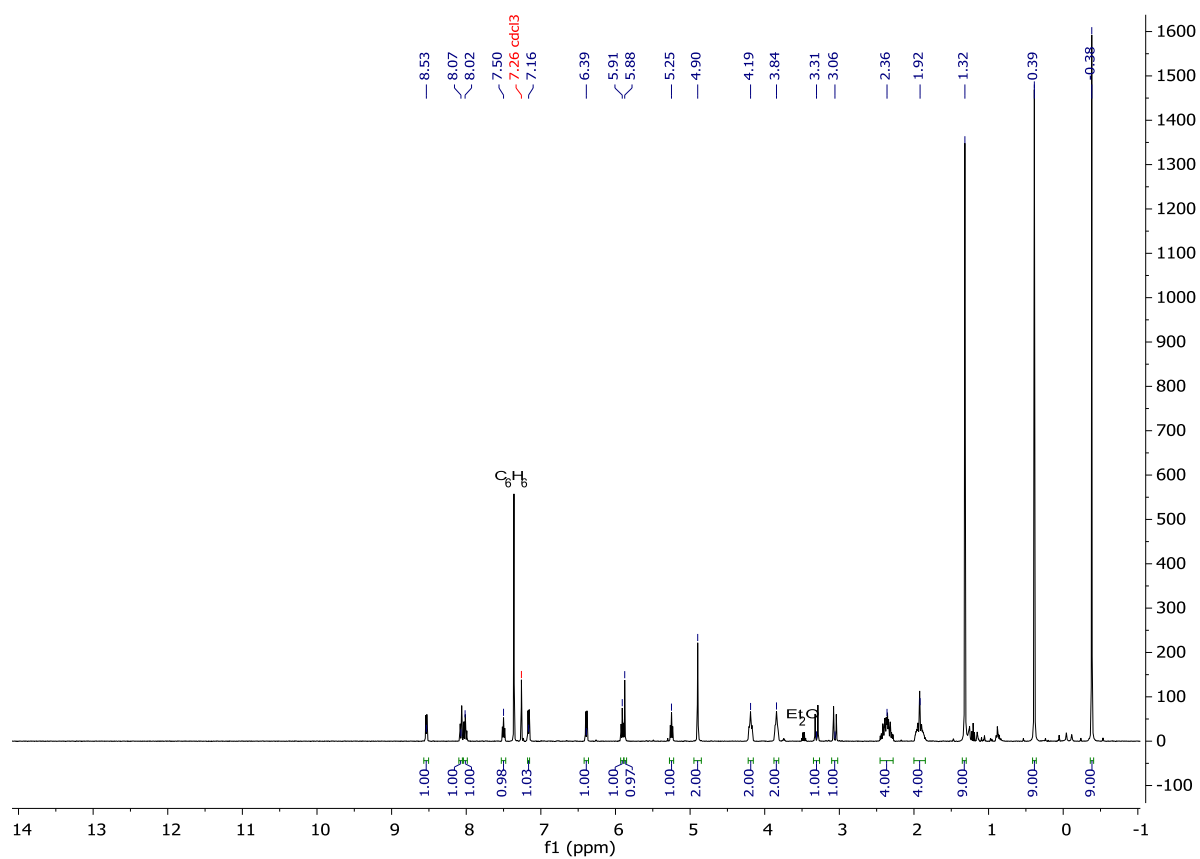Figure S6: ^{1}H NMR spectrum of **6**.

Figure S7: ^{1}H NMR spectrum of **7**. Cocrystallized benzene is marked as such in the sample (see also crystal structure).

b) ¹¹B NMR

Figure S8: ¹¹B NMR spectrum of **6**.

Figure S9: ¹¹B NMR spectrum of **7**.

c) ^{13}C{^{1}H} NMR
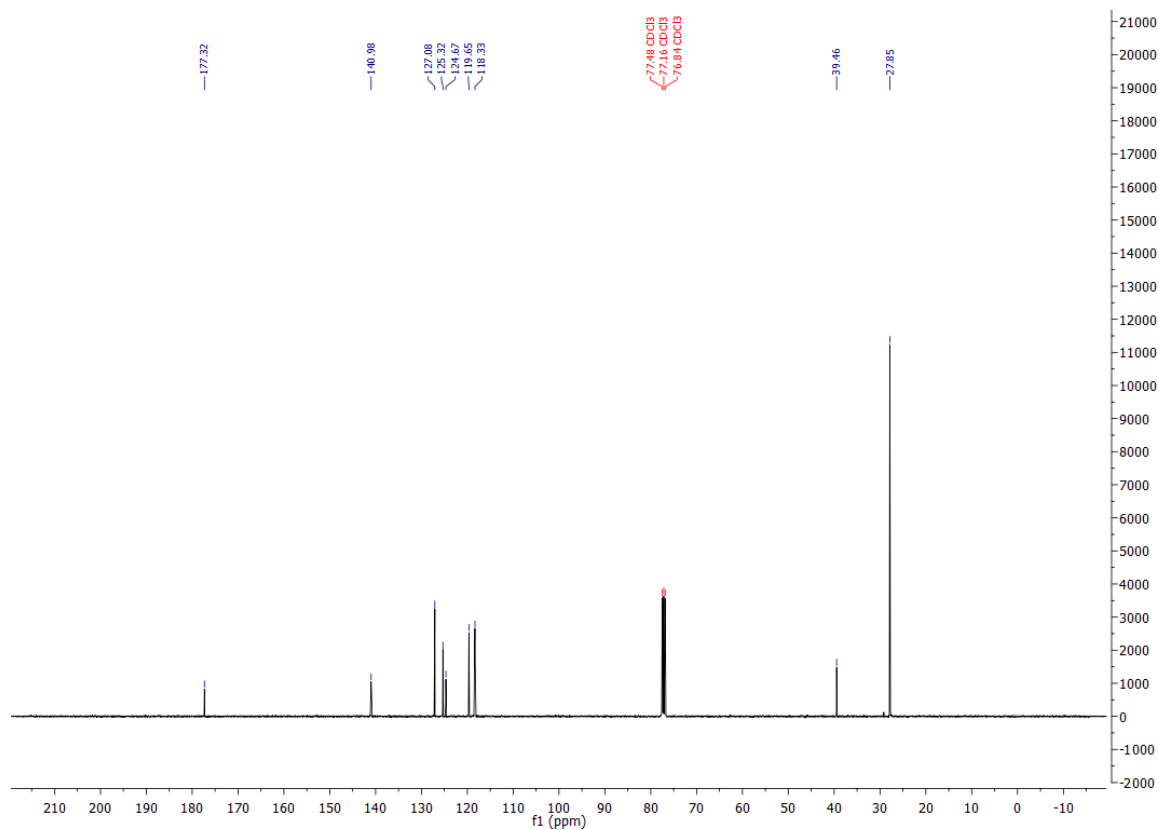
Figure S10: ^{13}C{^{1}H} NMR spectrum of N-(2-aminophenyl) pivalamid (**2**).
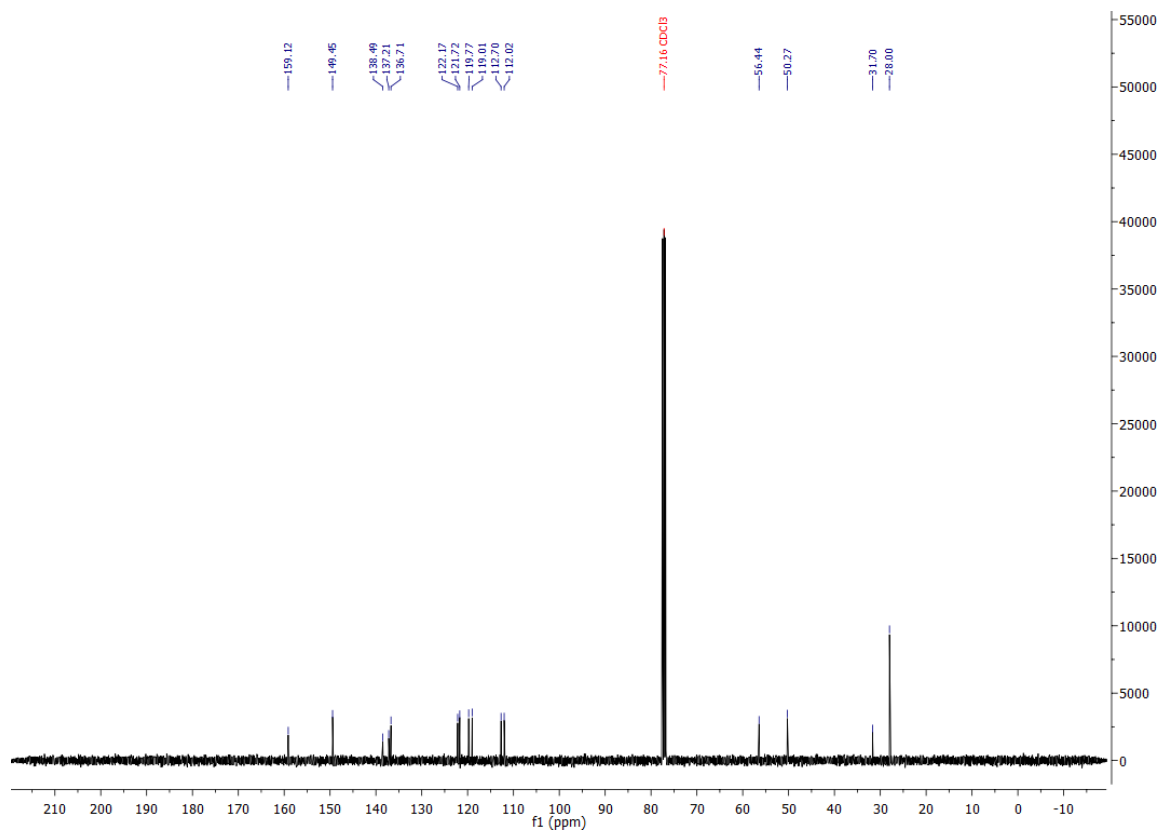
Figure S11: ^{13}C{^{1}H} NMR spectrum of N-neopentyl-N'-(pyridin-2-ylmethyl) phenylene diamine (**3**).
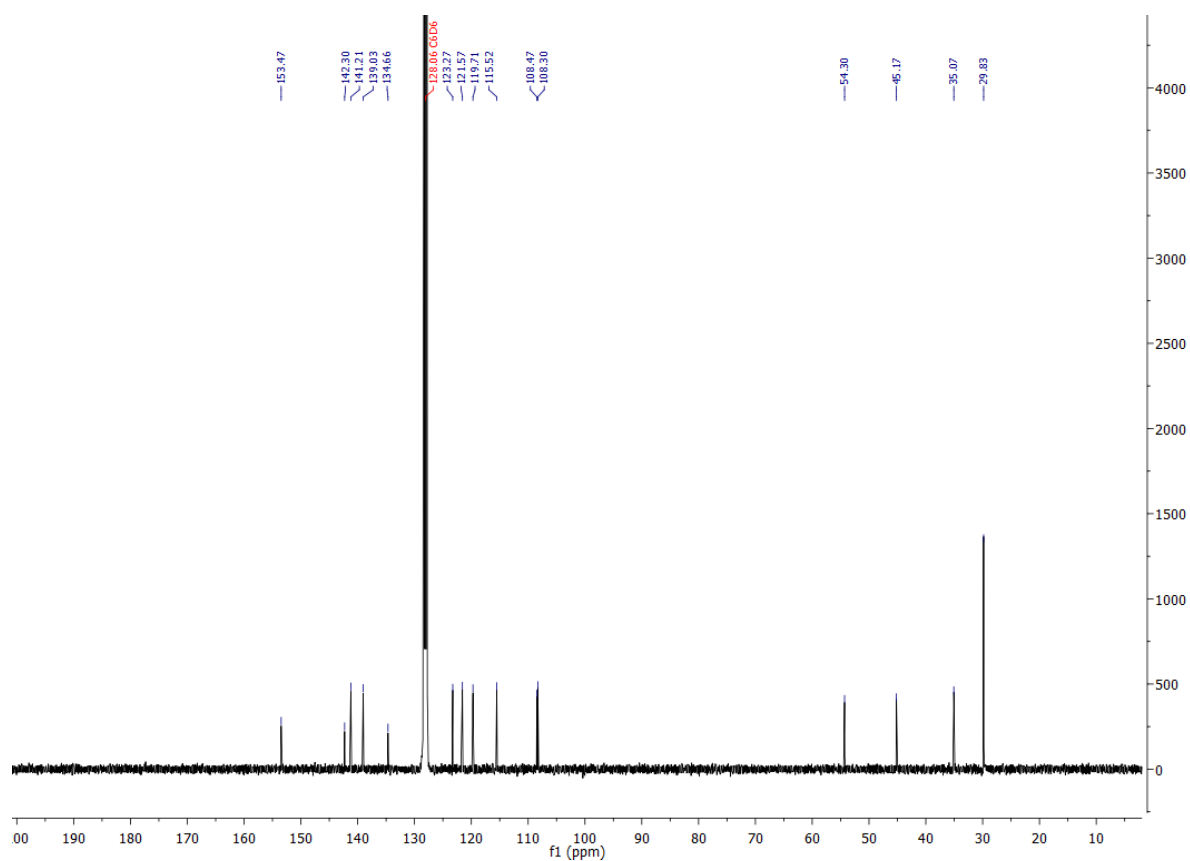
Figure S12: $^{13}C\{^1H\}$ NMR spectrum of 1-neopentyl-2,2-hydrochloro-3-((pyridin-2-yl)-methyl)-benzo[1,3,2] diazasilol (**4**).
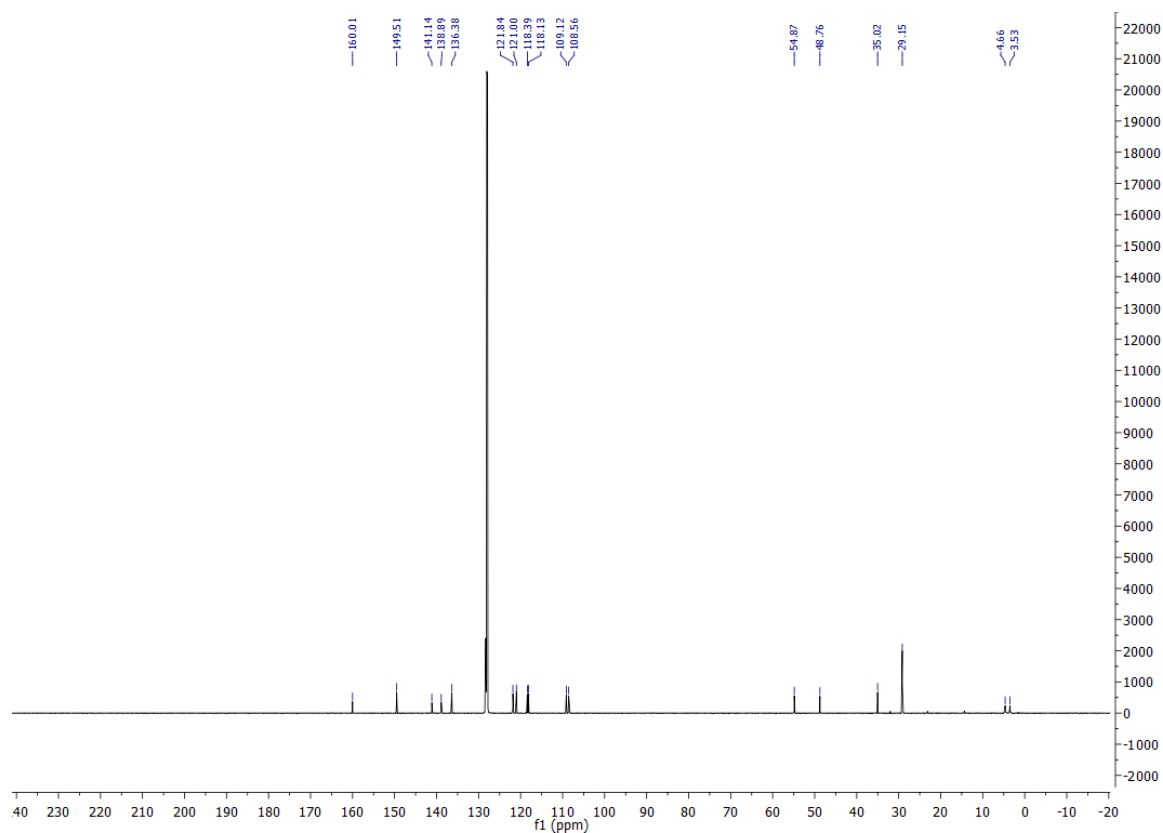
Figure S13: $^{13}C\{^1H\}$ NMR spectrum of 1-neopentyl-2-hydro-2-(bis-trimethylsilylamido)-3-((pyridin-2-yl)-methyl)-benzo[1,3,2] diazasilol (**5**).
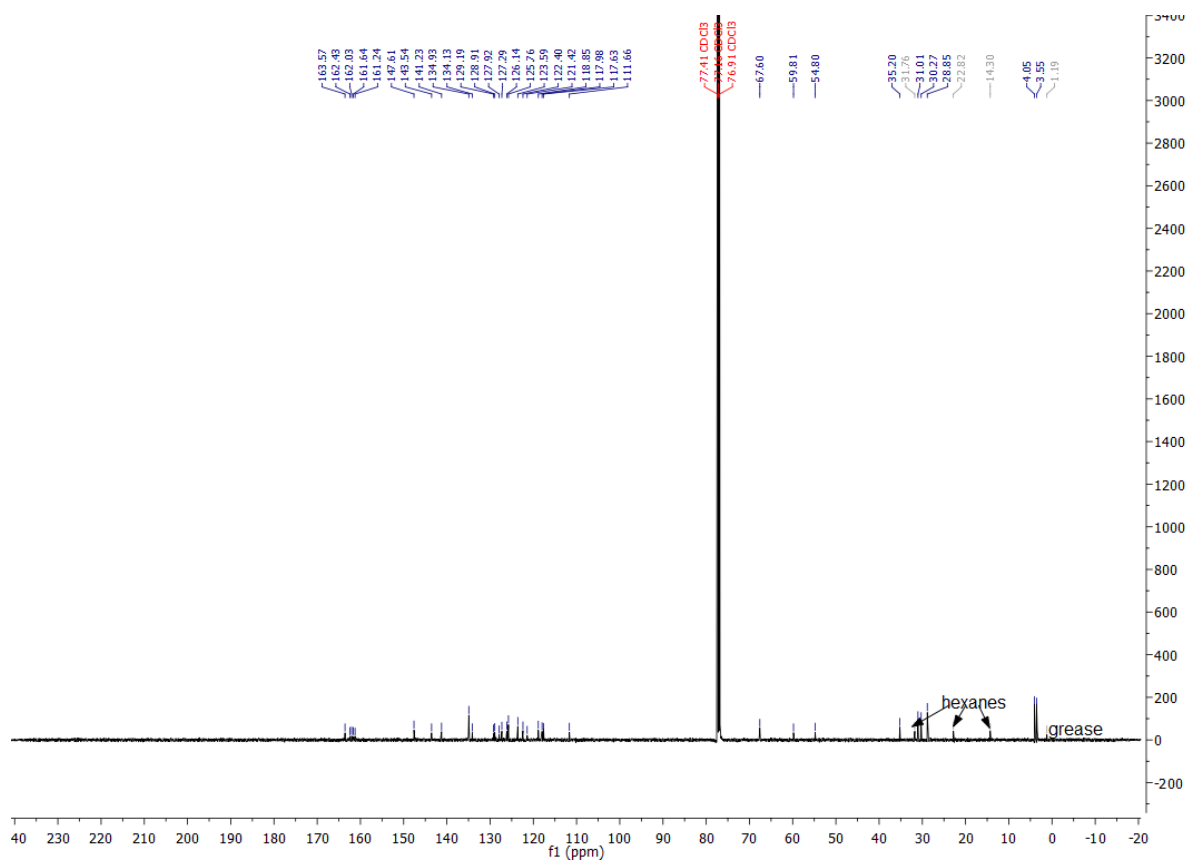
Figure S14: $^{13}C\{^1H\}$ NMR spectrum of **6**.
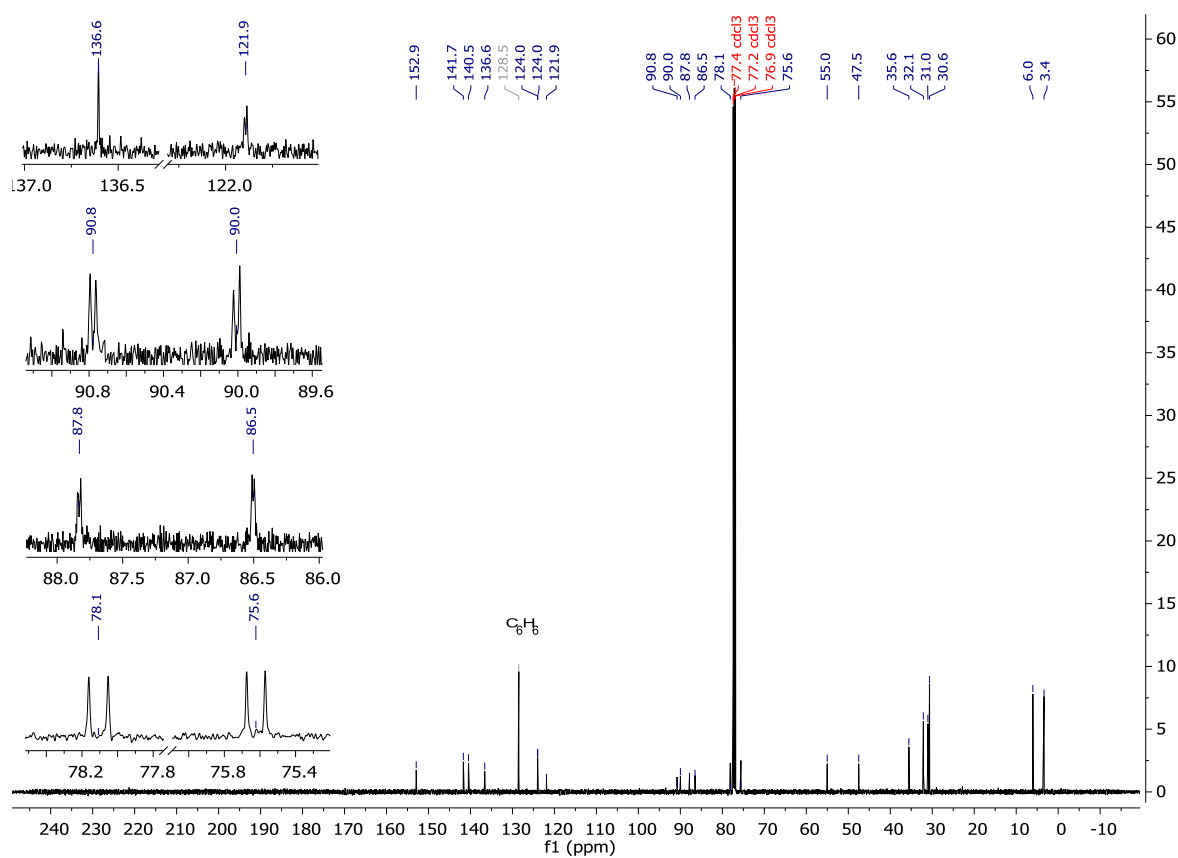
Figure S15: $^{13}C\{^1H\}$ NMR spectrum of **7**. Cocrystallized benzene is marked as such in the sample (see also crystal structure).
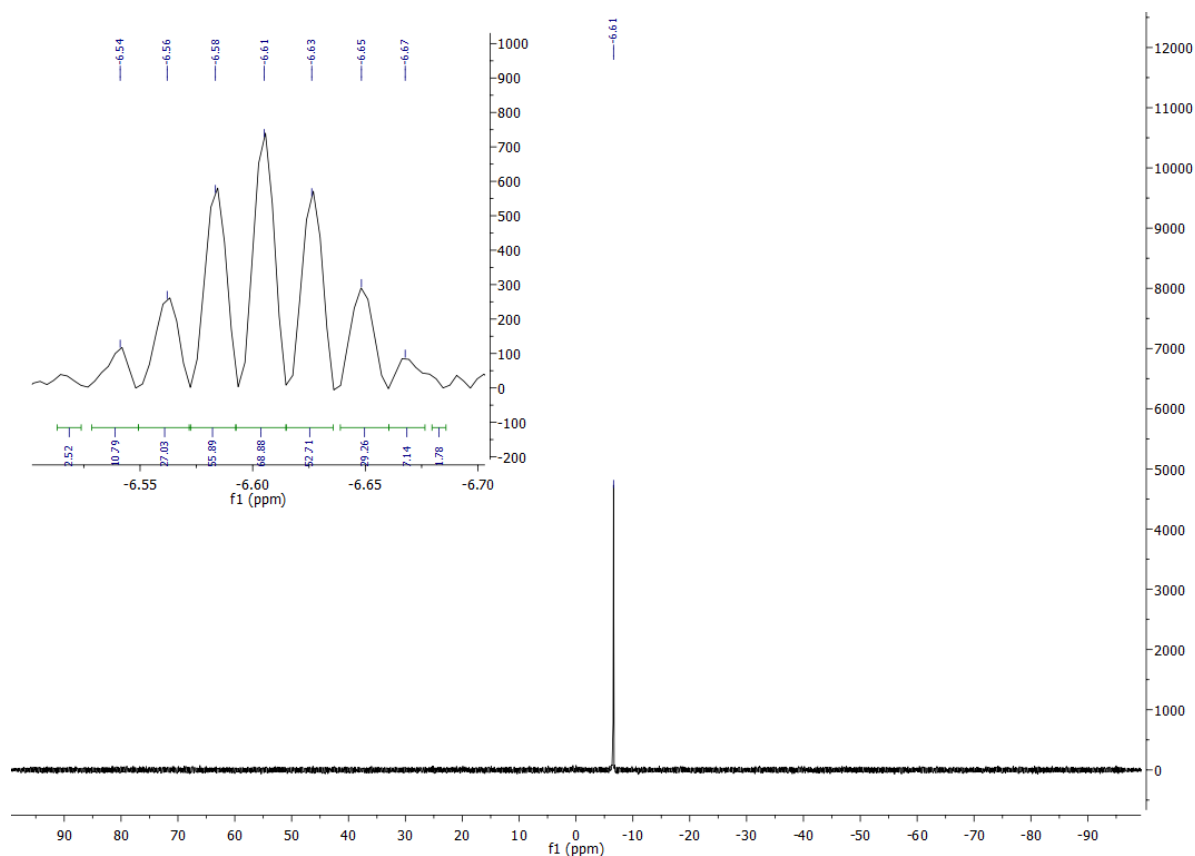
d) ¹⁹F{¹H} NMR
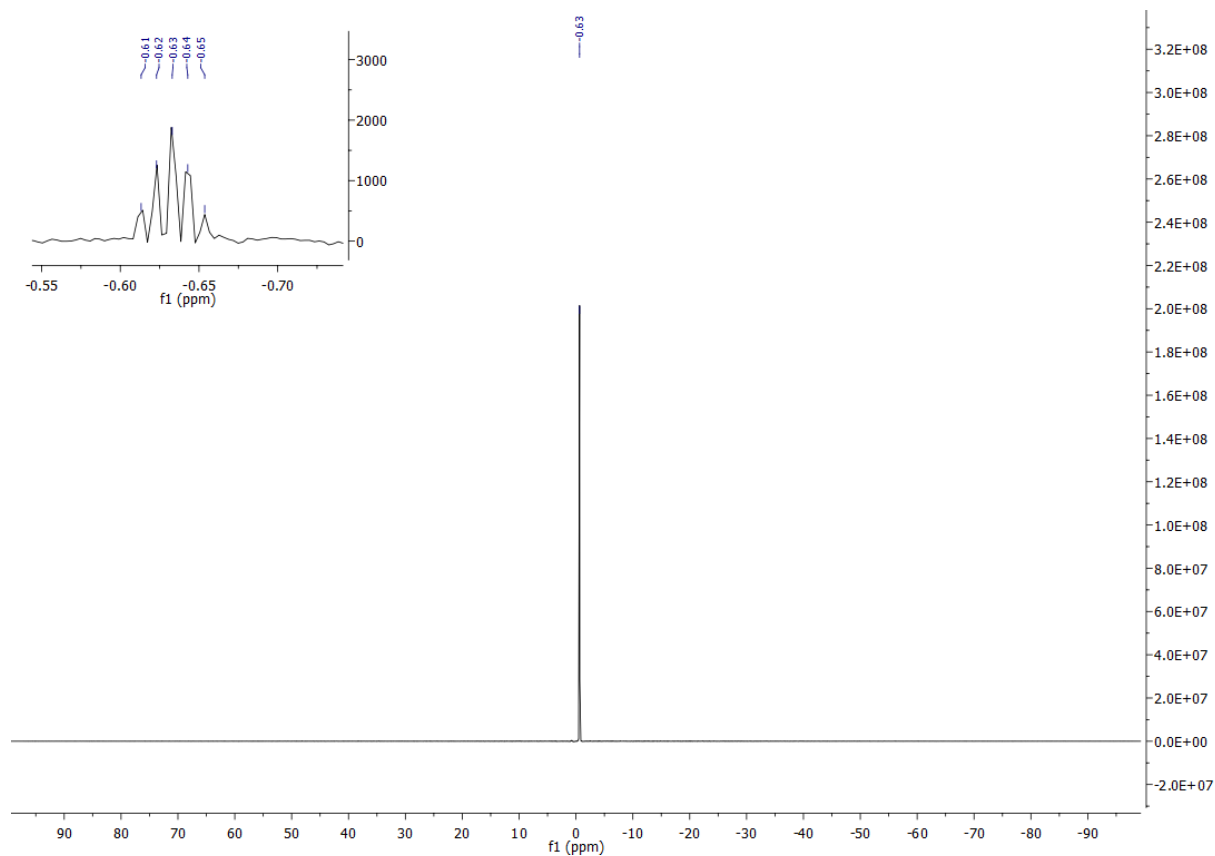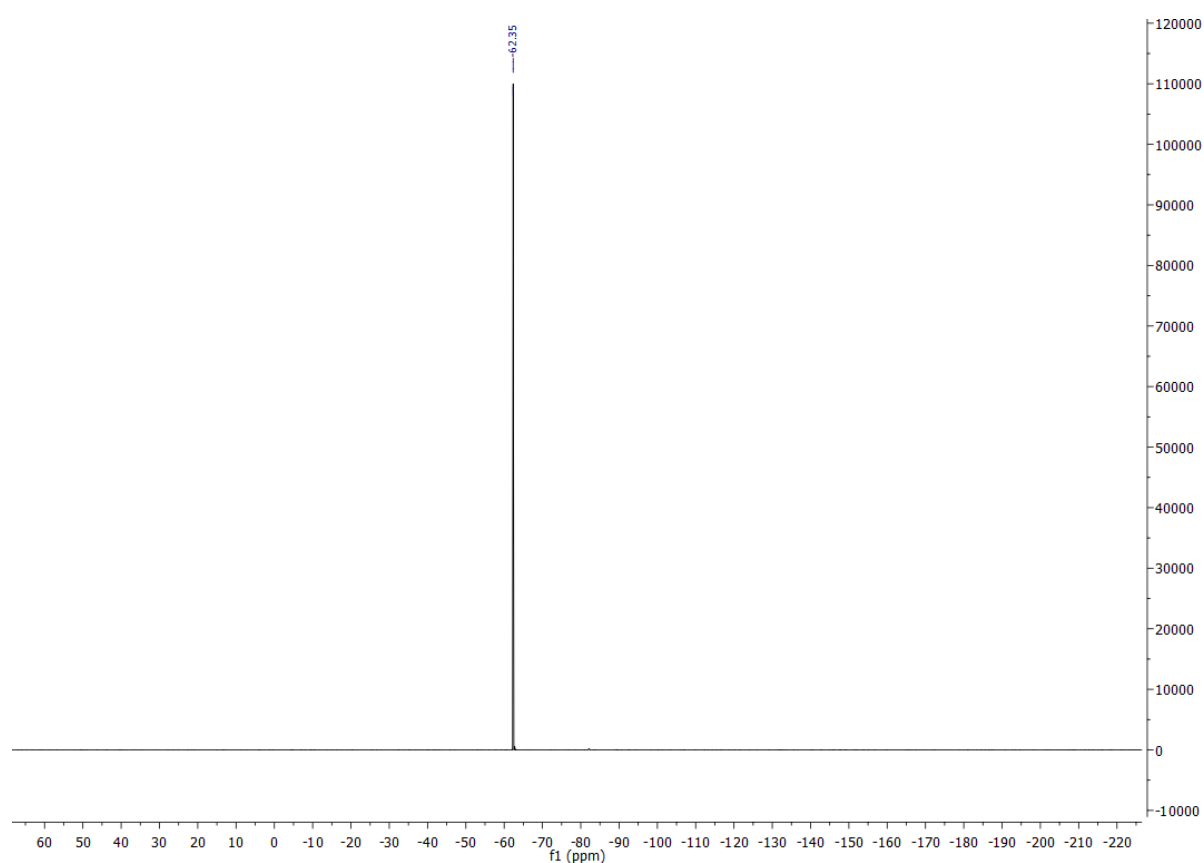

Figure S16: ¹⁹F{¹H} NMR spectrum of **6.**
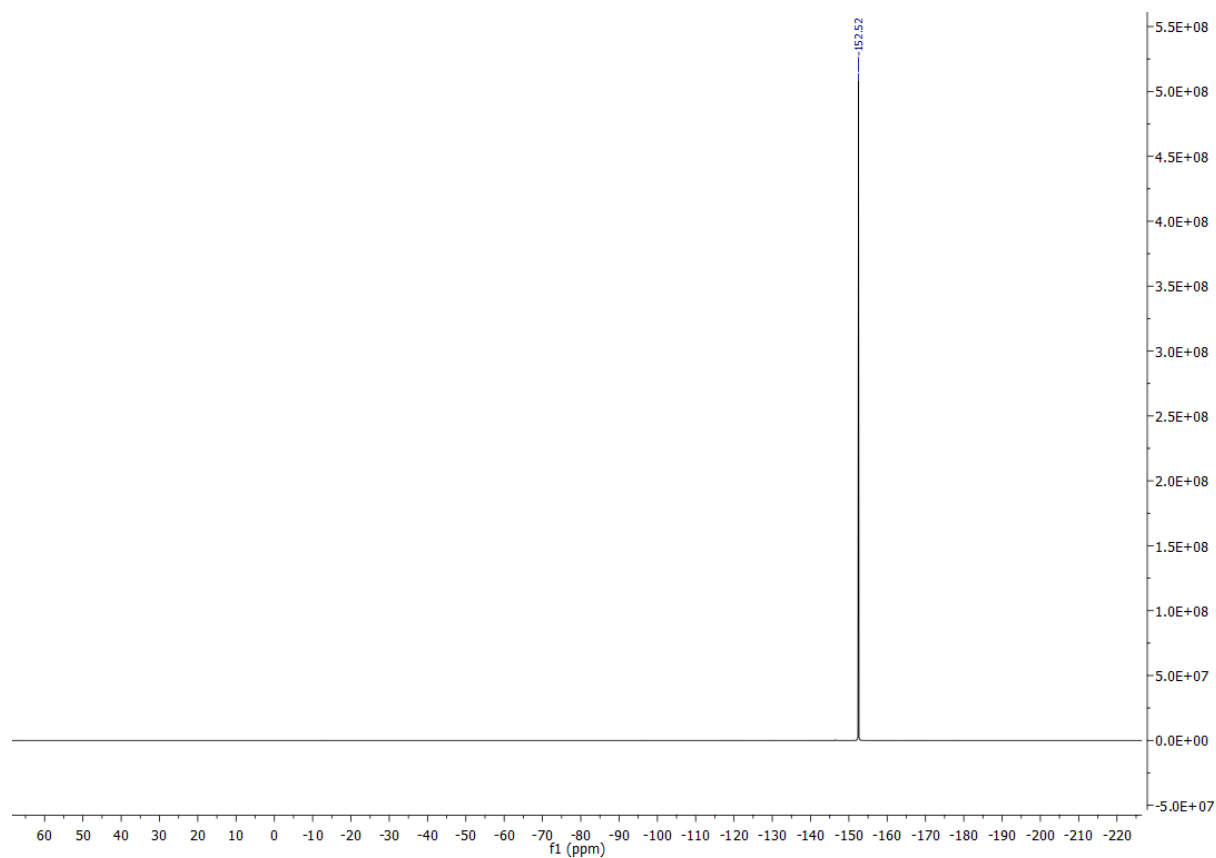
Figure S17: ¹⁹F{¹H} NMR spectrum of **7**.

e) ^{29}Si NMR
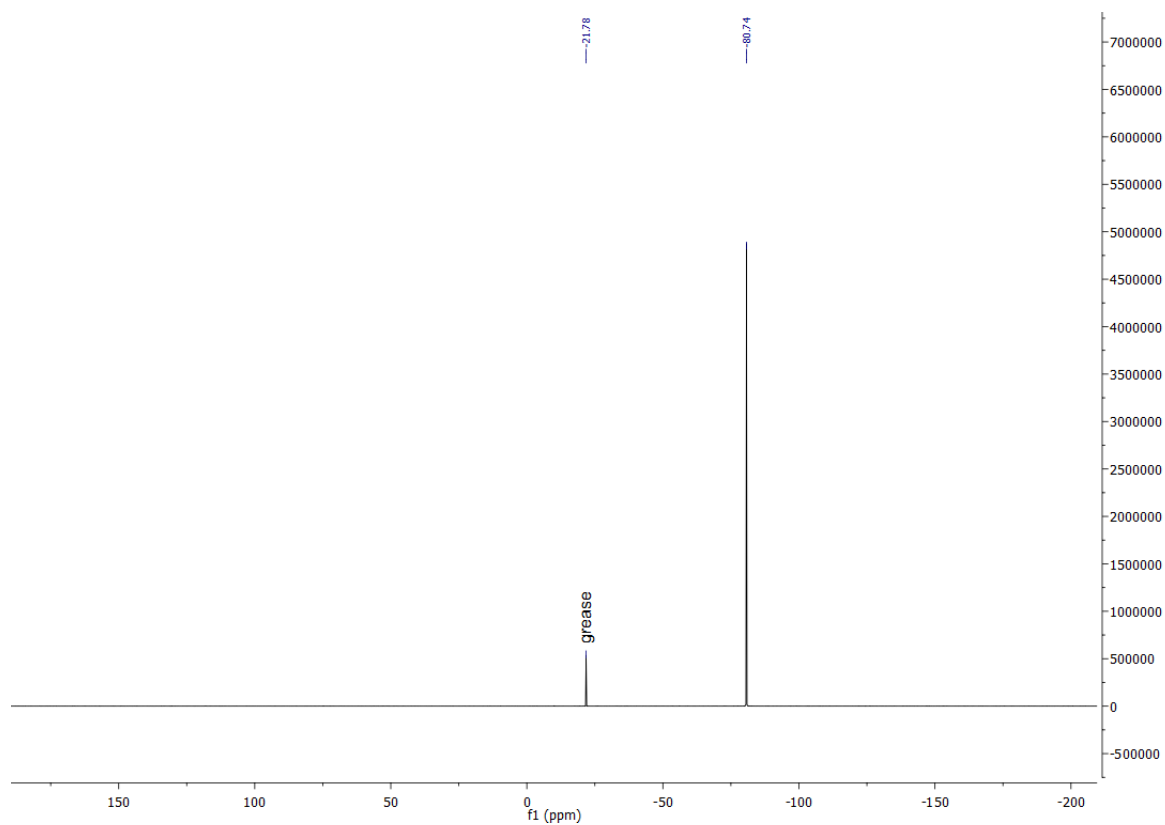
Figure S18: ^{29}Si{^{1}H} NMR spectrum of of 1-neopentyl-2,2-hydrochloro-3-((pyridin-2-yl)-methyl)-benzo[1,3,2] diazasilol (**4**).
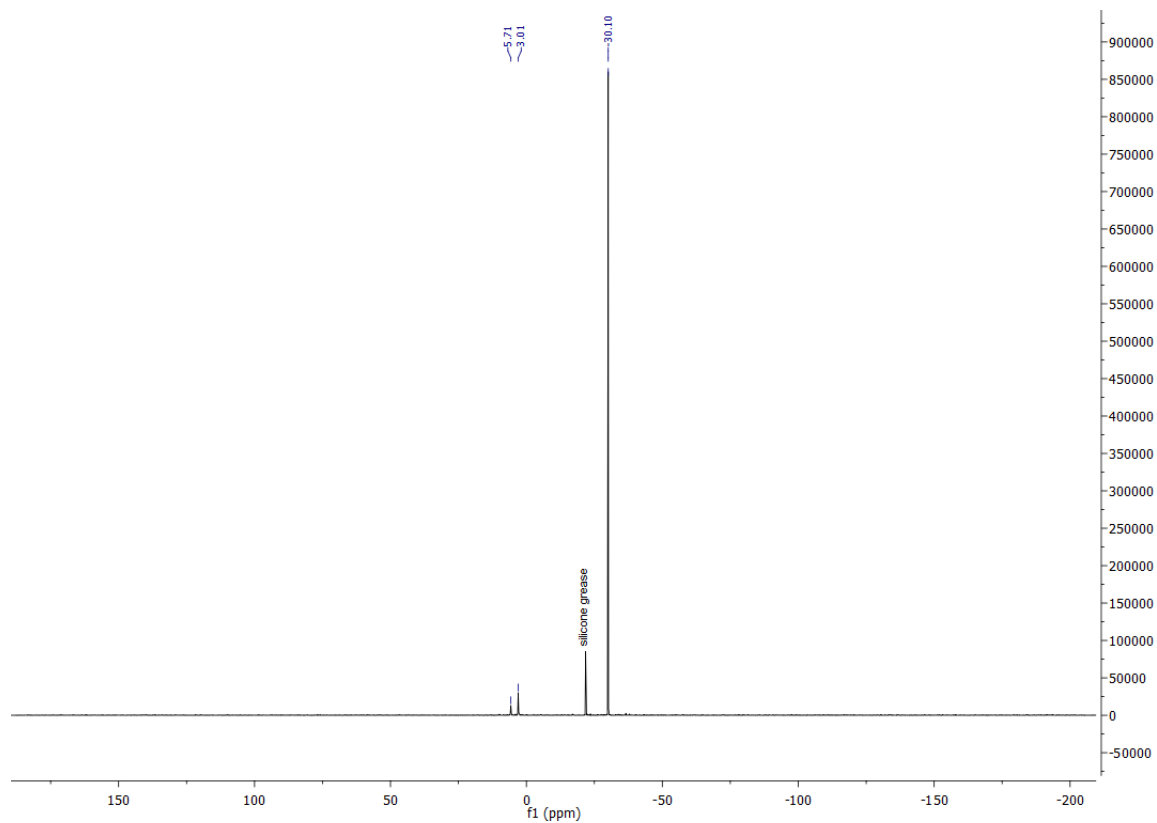
Figure S19: ^{29}Si{^{1}H} NMR spectrum of 1-neopentyl-2-hydro-2-(bis-trimethylsilylamido)-3-((pyridin-2-yl)-methyl)-benzo[1,3,2] diazasilol (**5**).
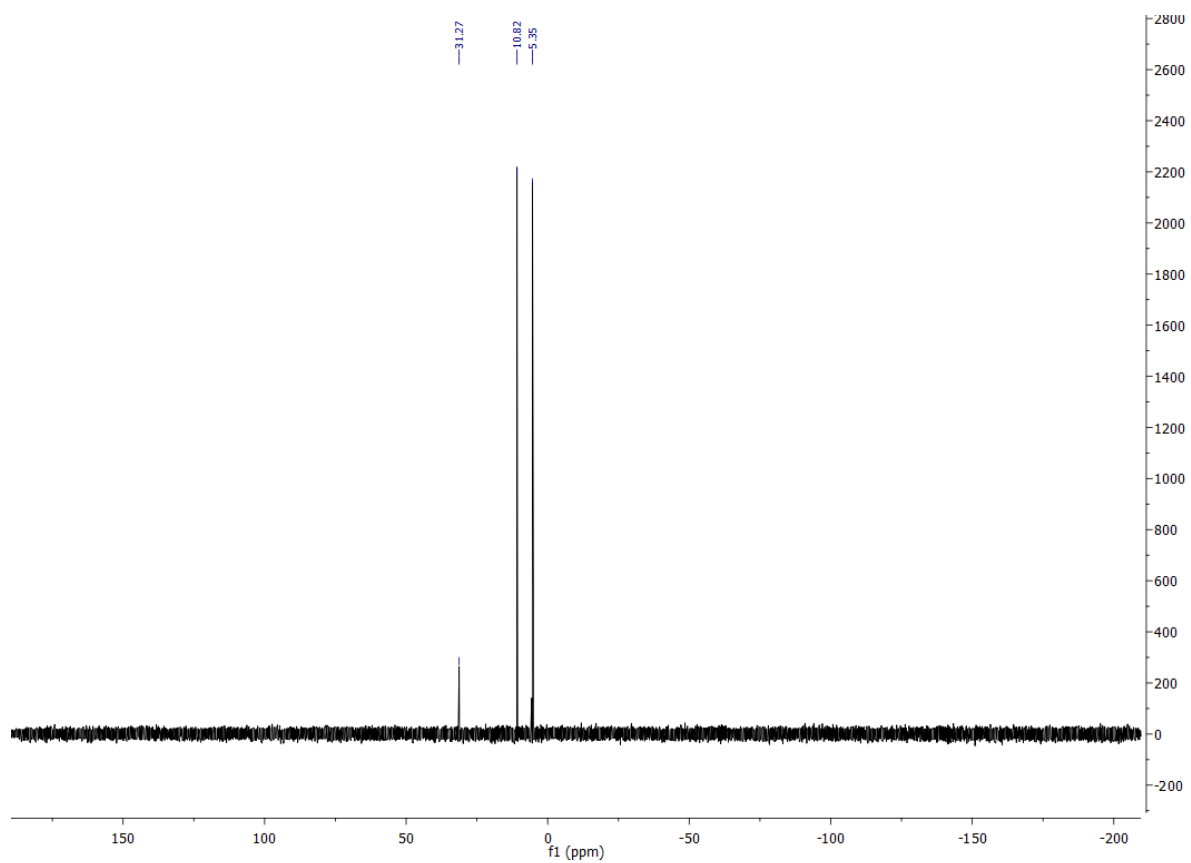
Figure S20: ^{29}Si{^{1}H} NMR spectrum of **6**.
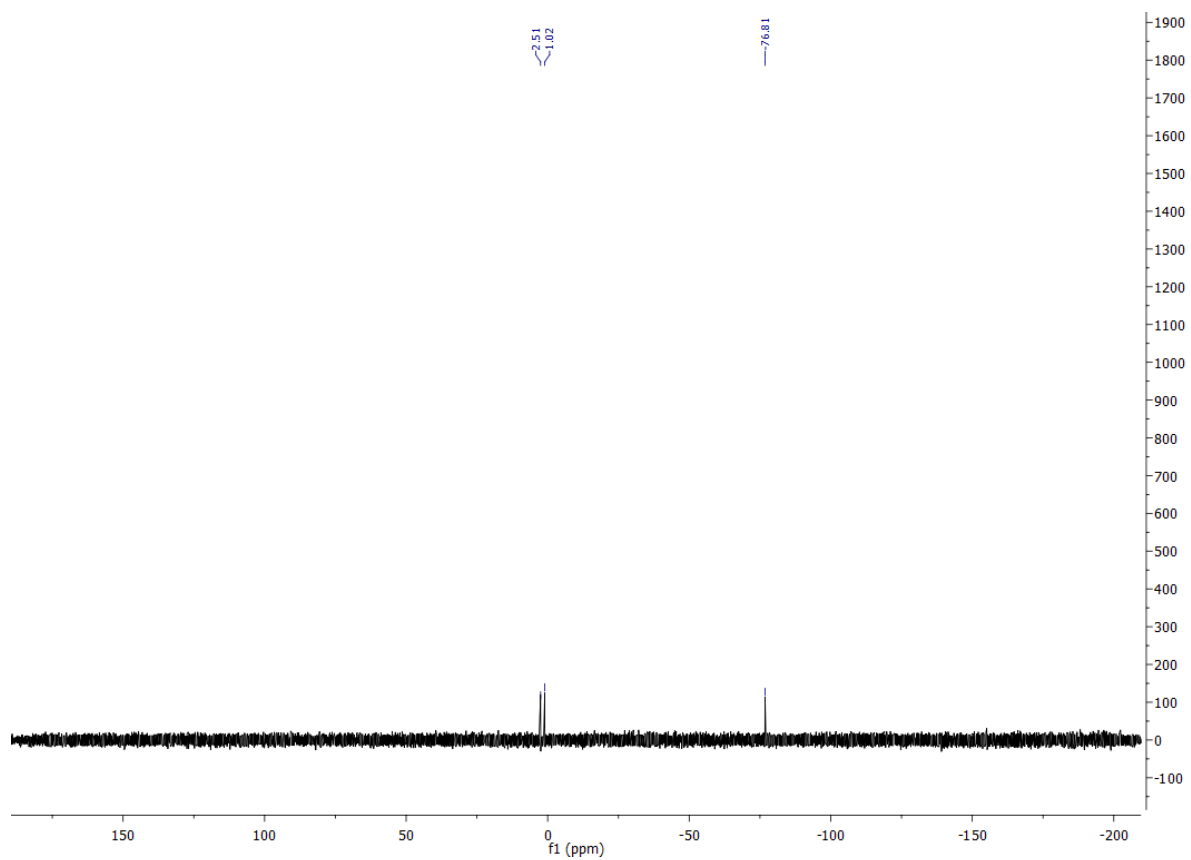
Figure S21: ^{29}Si{^{1}H} NMR spectrum of **7**.

2. ESI-MS
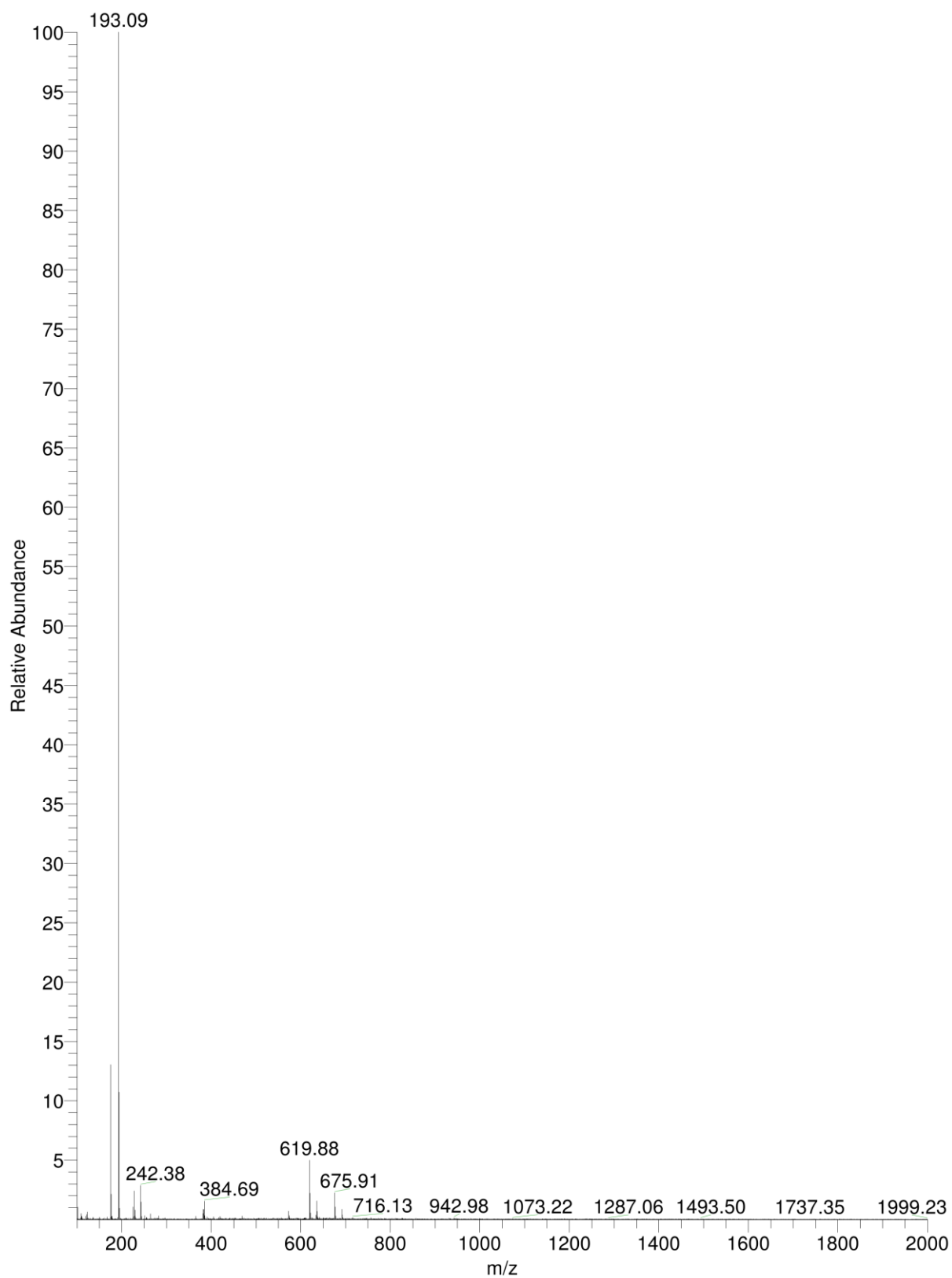
Figure S22: ESI MS of N-(2-aminophenyl) pivalamid (**2**).
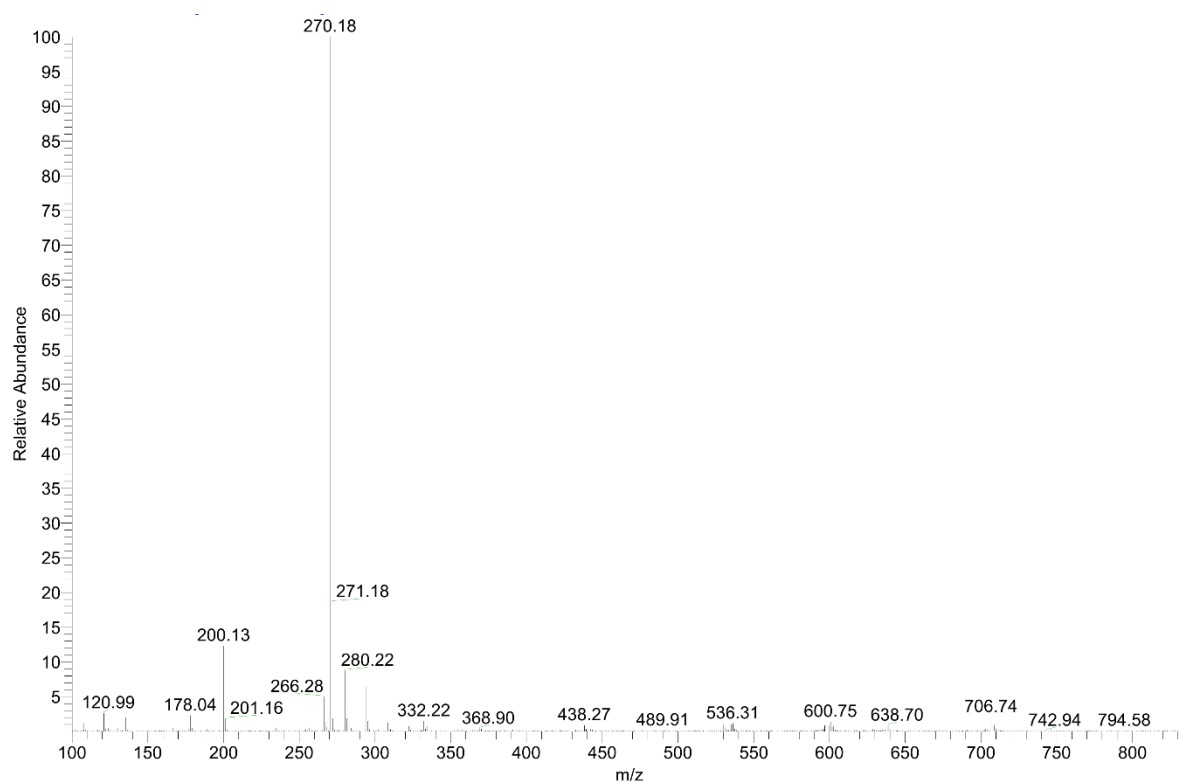
Figure S23: ESI MS of N-neopentyl-N'-(pyridin-2-ylmethyl) phenylene diamine (**3**).
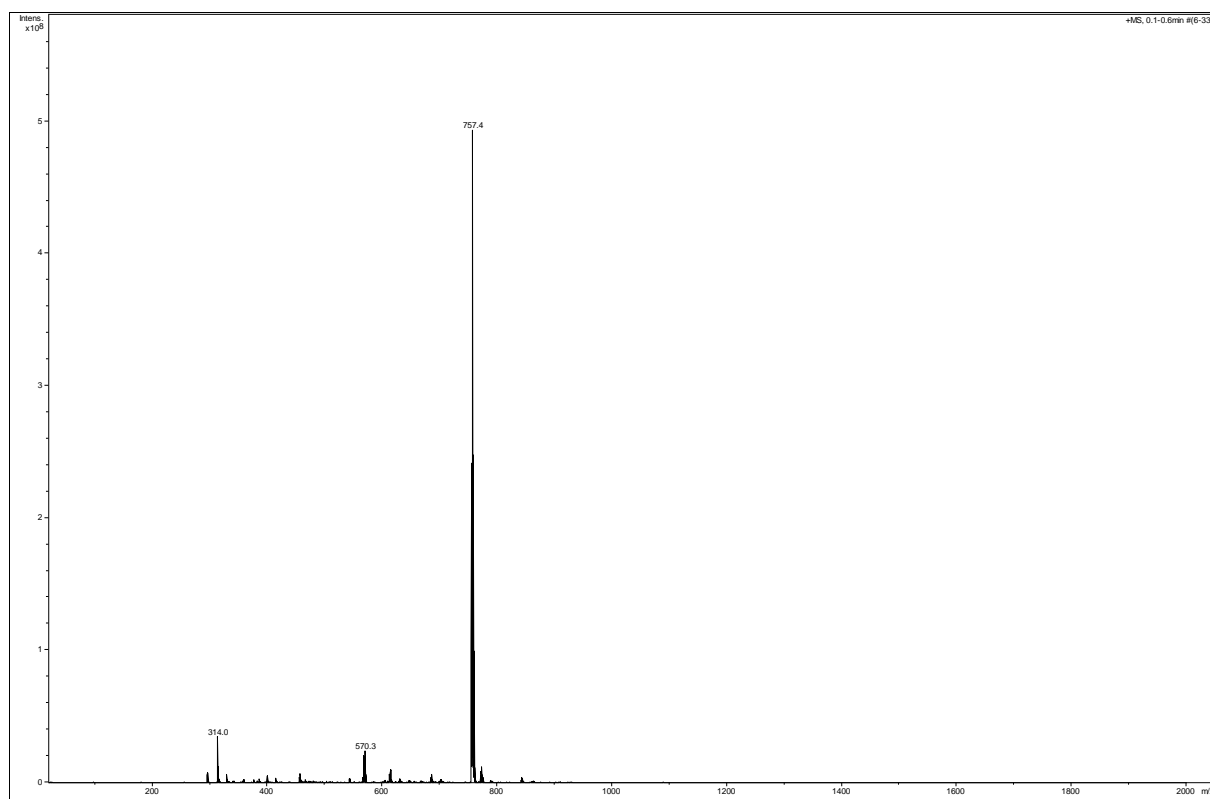
Figure S24: ESI MS of **6**.
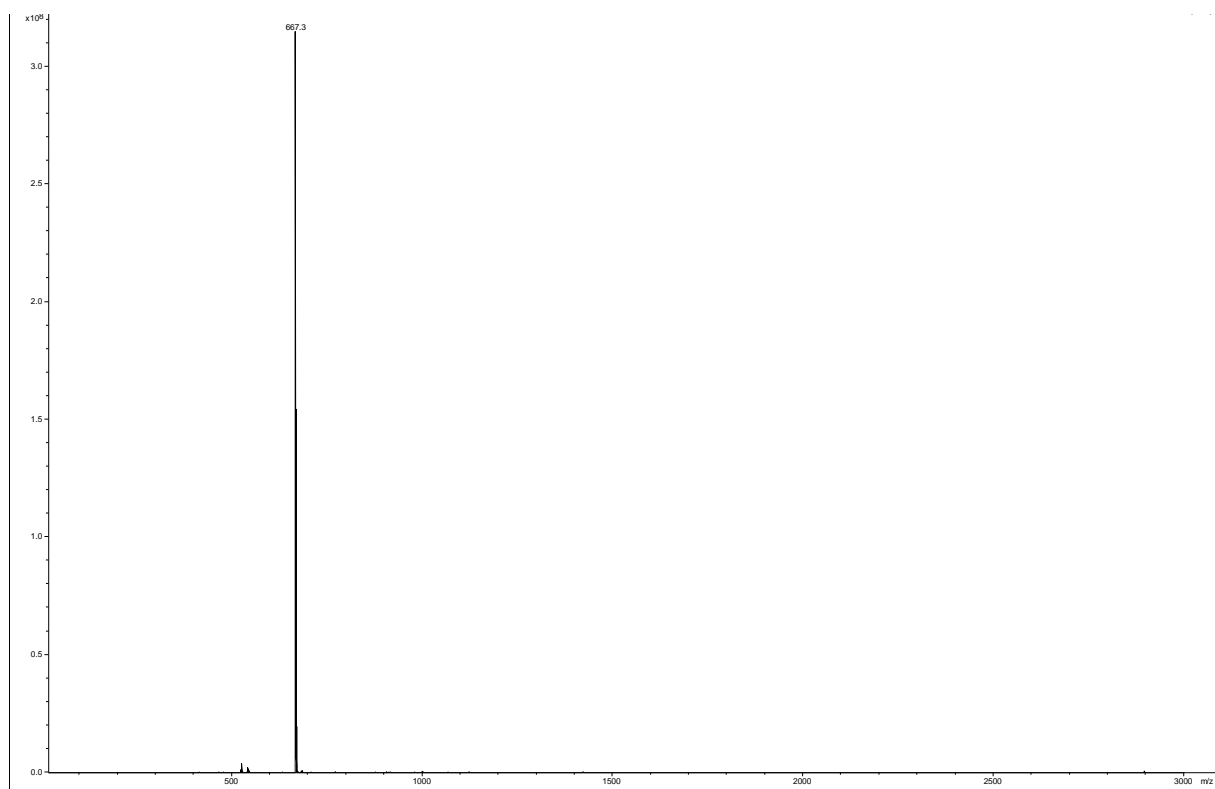
Figure S25: ESI MS of **7**.

3. LIFDI MS
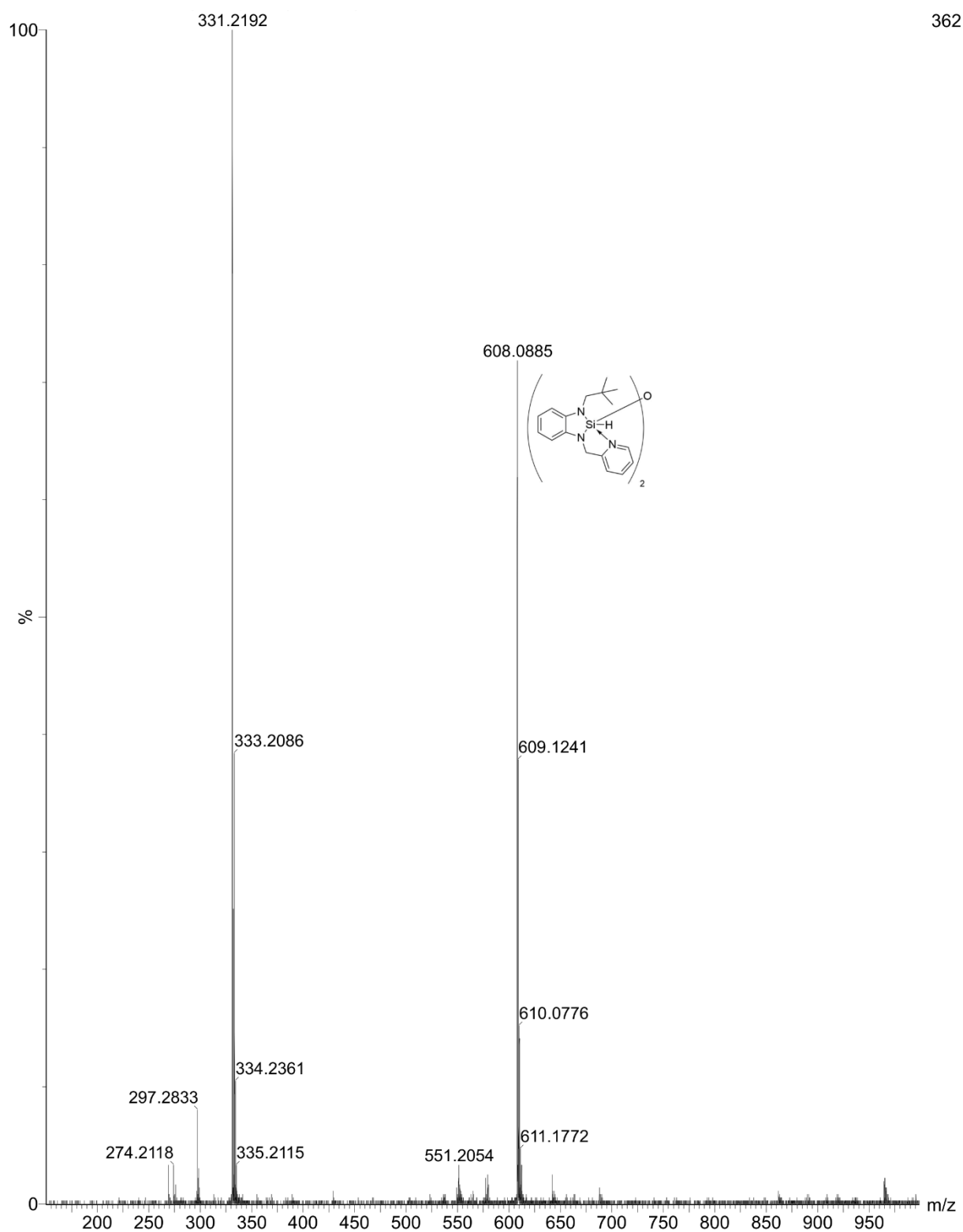
Figure S26: LIFDI MS of of 1-neopentyl-2,2-hydrochloro-3-((pyridin-2-yl)-methyl)-benzo[1,3,2] diazasilol (**4**). Additional signal at m/z=608 caused by hydrolysis product (hydrolysis with moisture in the course of the measurement).
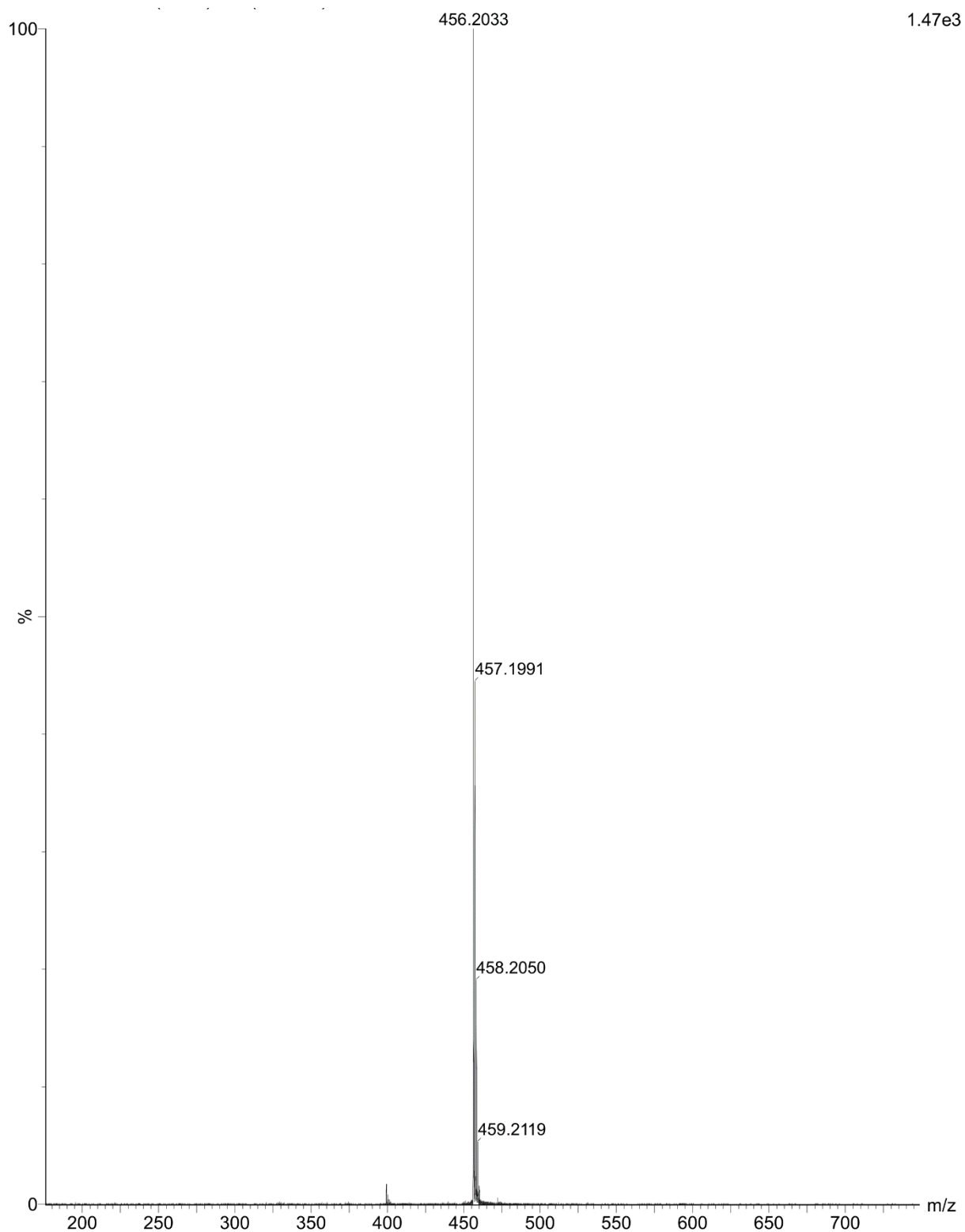
Figure S27: LIFDI MS of 1-neopentyl-2-hydro-2-(bis-trimethylsilylamido)-3-((pyridin-2-yl)-methyl)-benzo[1,3,2] diazasilol (**5**).

4. Single-crystal X-ray diffraction

a) X-Ray single crystal structure of *N*-neopentyl-*N'*-(pyridin-2-ylmethyl) phenylene diamine (**3**).
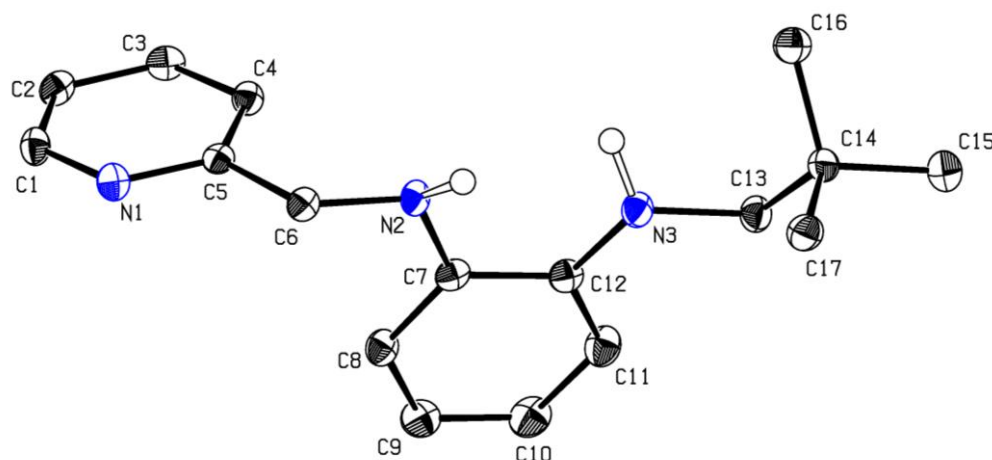
Figure S28: ORTEP style X-ray structure of **3**. Ellipsoids are shown at a 50% probability level. The hydrogen atoms are drawn with an arbitrary radius. Carbon-attached hydrogen atoms are omitted for clarity. Element colors: black – carbon, blue – nitrogen.

b) X-ray measurement details

Data were collected on an X-ray single crystal diffractometer equipped with a CCD detector (Bruker APEX II, κ-CCD), a rotating anode (Bruker TXS) with MoK$_\alpha$ radiation (λ = 0.71073 Å) and a Helios optic monochromator (**3**, **6**) or on a Bruker D8 Kappa APEX II system equipped with a fine-focused sealed tube with with MoK$_\alpha$ radiation (λ = 0.71073 Å) and a Triumph monochromator (**4**, **5**, **7**) by using the APEX software package.[1] The measurements were performed on a single crystal coated with perfluorinated ether. The crystal was fixed on top of a microsampler and transferred to the diffractometer. The crystal was frozen under a stream of cold nitrogen. A matrix scan was used to determine the initial lattice parameters. Reflections were merged and corrected for Lorentz and polarization effects, scan speed, and background using SAINT.[2] Absorption corrections, including odd and even ordered spherical harmonics were performed using SADABS.[2] Space group assignments were based upon systematic absences, E statistics, and successful refinement of the structures. Structures were solved by direct methods with the aid of successive difference Fourier maps, and were refined against all data using SHELXLE[3] in conjunction with SHELXL-2014[4]. Hydrogen atoms were assigned to ideal positions and refined using a riding model with an isotropic thermal parameter 1.2 times that of the attached carbon atom (1.5 times for methyl hydrogen atoms). Silicon- and nitrogen-attached protons could be located on the difference Fourier maps and were allowed to refine freely. If not mentioned otherwise, non-hydrogen atoms were refined with anisotropic displacement parameters. Full-matrix least-squares refinements were carried out by minimizing $\Sigma w(F_o^2-F_c^2)^2$ with SHELXL-97[5] weighting scheme. Neutral atom scattering factors for all atoms and anomalous dispersion corrections for the non-hydrogen atoms were taken from International Tables for Crystallography.[6] Images of the crystal structures were generated by PLATON.[7]

c) Crystallographic data

Table S1: Crystallographic data for compounds **3**, **4**, **5**, **6** and **7**.

	3	**4**	**5**	**6**	**7**
formula	$C_{17}H_{23}N_3$	$C_{17}H_{22}ClN_3Si$	$C_{23}H_{40}N_4Si_3$	$C_{63}H_{64}BF_{24.07}Ir$ N_4Si_3	$C_{23}H_{33.5}B_{0.5}F_2$ $N_2Rh_{0.5}Si_{1.5}$
M_r	269.38	331.91	456.86	1621.71	475.01
crystal habit	clear colorless fragment	clear yellow fragment	clear colorless fragment	clear orange fragment	clear yellow fragment
crystal system	monoclinic	triclinic	triclinic	monoclinic	triclinic
space group	$P21/n$	$P\bar{1}$	$P\bar{1}$	$C2/c$	$P\bar{1}$
a [Å]	9.1143(5)	11.463(2)	9.657(2)	19.308(2)	11.591(4)
b [Å]	5.6876(3)	12.121(1)	10.800(1)	18.256(1)	12.932(5)
c [Å]	29.019(2)	13.285(2)	14.678(2)	40.759(3)	18.375(7)
α [°]	90	77.296(4)	77.297(6)	90	108.43(2)
β [°]	97.306(2)	77.546(4)	86.511(6)	101.562(2)	99.56(2)
γ [°]	90	71.924(4)	63.939(5)	90	104.37(2)
V [Å^3]	1492.1(2)	1690.1(3)	1340.4(3)	14076(2)	2440(2)
Z	4	4	2	8	4
ρ_c	1.199	1.304	1.132	1.531	1.293
F (000)	584	704	496	6485	998
T [K]	100(2)	100(2)	100(2)	100(2)	100(2)
μ [mm^{-1}]	0.072	0.297	0.194	2.053	0.474
data/restraints/ parameters	2733/0/192	8379/0/411	7477/0/284	12417/319/991	8589/491/652
GoF (F^2)	1.047	1.076	1.071	1.050	1.068
$R_1{}^a$, $wR_2{}^b$ ($I >$ $2\sigma(I)$)	0.0378, 0.0848	0.0328, 0.0852	0.0287, 0.0838	0.0500, 0.0987	0.0326, 0.0787
R_1, wR_2 (all data)	0.0527, 0.0901	0.0397, 0.0887	0.0316, 0.0904	0.0859, 0.1070	0.0406, 0.0831
R_{int}	0.0648	0.0347	0.0276	0.1517	0.0454
CCDC number	1571194	1571192	1571193	1571196	1571195

5. Thermodynamic parameters from VT NMR

For the determination of the thermodynamic parameters of the rotation barrier around Si1–N4 in **5**, a NMR spectra were recorded at various temperatures in THF-d_8.

The overcoming of the rotational barrier in molecule **5** can be described as a first-order kinetic process. As such, the conformer lifetime τ is reciprocally proportional to the rate constant k.

According to Arrhenius, the rate constant k is given by:

$$k = A \cdot e^{\frac{E_A}{RT}}$$

Following the relations for Gibbs free activation enthalpy, require standard pressure and apply the natural logarithm, for the first order reaction at temperature T it can be denoted:

$$\ln\frac{k}{T} = \frac{\Delta H}{R} \cdot \frac{1}{T} + \frac{\Delta S}{R} + \ln\frac{k_B}{h}$$

(ΔH: activation Enthalpy; ΔS: activation entropy; k_B: Boltzmann constant; h: Planck constant; R: gas constant)

Thus, plotting $\ln\frac{k}{T}$ versus $\frac{1}{T}$ will makes all thermodynamic values accessible through slope or intercept.

E_A can eventually be calculated by

$$E_A = \Delta H + RT$$

Determination of reaction constant k:

At low temperatures (≤ 20 °C), the exchange rate was considered slow, and thus, with $w_{\frac{1}{2}}$ as the band width at half intensity level:

$$k = \frac{1}{\tau} = \pi \cdot w_{\frac{1}{2}}$$

Thereby, the linewidth at -40 °C was considered as "natural linewidth" without exchange and was substracted from the linewidths, measured at higher temperatures in order to reveal the exchange-related linewidths.

Around the coalescence point (20 − 45 °C), k was calculated through ($\Delta\delta$: separation between the two SiMe$_3$ signals in Hz):

$$k = \frac{1}{\tau} = \frac{\pi \cdot \Delta\delta}{\sqrt{2}}$$

For fast exchange at elevated temperatures (> 45 °C), k was calculated as ($\Delta\delta_{-40}$: line separation at -40 °C):

$$k = \frac{1}{\tau} = \frac{\pi \cdot \Delta\delta_{-40}^2}{2w_{\frac{1}{2}}}$$

Table S2: Measured and calculated parameters within the VT ^{1}H NMR studies of **5**.

T	w_1/2	Δδ	k	1/T	ln(k/T)
-40	2,51	157,4	0,1	0,00428908	
-20	2,66	148,4	0,46338492	0,00395023	-6,30317942
0	4,71	140	6,9272118	0,00366099	-3,6745637
20	28,55	127,8	81,8243515	0,00341122	-1,27610953
40	74,28	92	204,372615	0,00319336	-0,42673744
45	145,0	78	173,272435	0,00314317	-0,60765785
47	128,5	62	305,834199	0,00312354	-0,04574651

ln(k/T) = -7250,8 (1/T) + 22,7
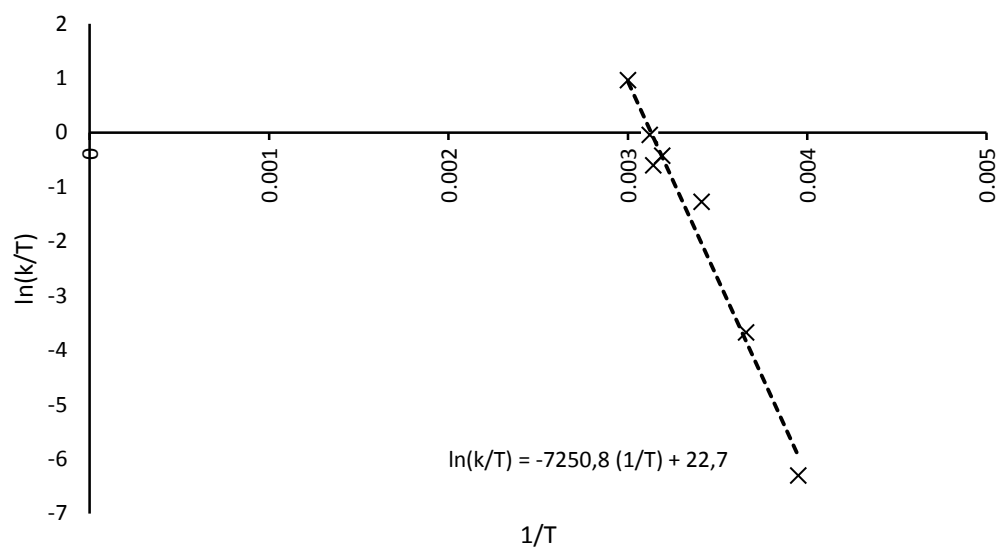
Figure S28: Linear Regression of ln(k/T) vs. 1/T.

Linear regression and calculation of the parameters reveals:

$$\Delta H = 60.3 \frac{kJ}{mol}; \Delta S = -8.8 \frac{J}{mol \cdot K} ; E_A = 62.9 \frac{kJ}{mol}$$

6. References

1. *APEX suite of crystallographic software, APEX 2, version 2008.4.*, Bruker AXS Inc., Madison, Wisconsin, USA (2008).

2. *SAINT, version 7.56a, SADABS, version 2008.1*, Bruker AXS Inc., Madison, Wisconsin, USA (2008).

3. Hübschle, C. B.; Sheldrick, G. M.; Dittrich, B. *SHELXLE, J. Appl. Crystallogr.* 2011, **44**, 1281-1284.

4. Sheldrick, G. M. *SHELXL-2014*, University of Göttingen, Göttingen, Germany (2014).

5. Sheldrick, G. M. *SHELXL-97*, University of Göttingen, Göttingen, Germany (1998).

6. Wilson, A. J. C. *International Tables for Crystallography*, Dordrecht, The Netherlands, Kluwer Academic Publishers (1992).

7. A. L. Spek, *Acta Cryst. D*, 2009, **65**, 148-155.

8. P. W. Atkins and J. de Paula, Physical Chemistry (7th ed.) (Oxford University Press, Oxford, UK, 2002).

9. H. Günther, NMR spectroscopy: basic principles, concepts, and applications in chemistry (2nd ed.) (John Wiley & Sons, New York, 1996)

10. R. J. Silbey, R. A. Alberty, and M. G. Bawendi, Physical Chemistry (4th ed.), (Wiley, New York, 2004)

11. R. C. Neuman Jr.; V. Jonas, *J. Org. Chem.* 1974, **39**, 925-928.

12. https://www.csun.edu/~jeloranta/CHEM352L/experiment3.pdf, 01.10.2017; 17:35 MESZ

13. J. A. Weil, J. R. Bolton, and J. E. Wertz, Electron paramagnetic resonance: elementary theory and practical applications (John Wiley & Sons, New York, 1994).